Short communication

Regional dependency of the vascular smooth muscle cell contribution to the mechanical properties of the pig ascending aortic tissue

Dominique Tremblay [a,b], Raymond Cartier [b], Rosaire Mongrain [c,b], Richard L. Leask [a,b,*]

[a] Department of Chemical Engineering, McGill University, Wong Building, 3610 University Street, Montreal, Quebec, Canada H3A 2B2
[b] Montreal Heart Institute Research Centre, Montreal, Canada
[c] Department of Mechanical Engineering, McGill University, Montreal, Canada

ARTICLE INFO

ABSTRACT

Background: Dilation and dissection of aneurysmal ascending aortic tissues occur preferentially at the outer curvature of the vessel. In this study we hypothesize that the density and contractile properties of the vascular smooth muscle cells (VSMCs) of the pig ascending aorta (AA) are heterogeneous and could explain the non-uniform remodeling and weakening of the AA during aneurysm formation.
Methods: Eleven pig AA rings were collected. Two square samples of 15×15 mm were taken from each ring from the inner and outer curvature of the AA. Each sample was subjected to equi-biaxial tensile testing in Krebs–Ringer solution maintained at 37 °C. Each test consisted of 8 cycles of preconditioning followed by one experimental run from 0% to 30% strain. Phenylephrine (10^{-5} M) was added to contract VSMCs. After biaxial testing, samples were paraffin-embedded and stained with hematoxylin–phloxine–saffron (HPS) to quantify VSMC density.
Results: Significant differences in cell density, maximum contractile stress resultant magnitude (MCSRM) and orientation (θ_{MCSR}) were found between the inner and outer curvature. The inner curvature had the greatest contraction. The outer curvature had the highest VSMC density with the maximum contraction stress resultant oriented towards the axial direction.
Conclusion: VSMC activation with phenylephrine had a significant effect on the stiffness of the pig AA. This effect was independent of location and direction. However, cell orientation, density and contractile properties were dependent on location and suggest variations in the remodeling capabilities, tissue strain and cell phenotype between locations.

Crown Copyright © 2010 Published by Elsevier Ltd. All rights reserved.

1. Introduction

Aneurysm formation in the ascending aorta (AA) results from tissue remodeling, which changes the tissue mechanical properties (Choudhury et al., 2009). This remodeling does not occur uniformly around the AA (Corte et al., 2006; Cotrufo et al., 2003). Dilation, dissection and rupture are most pronounced at the outer curvature of the AA (Desai et al., 2007; Gomez et al., 2009) suggesting that a non-uniform remodeling and weakening of the vessel exist during aneurysm formation, in particular at the outer curvature.

Remodeling of the AA is produced largely by vascular smooth muscle cells (VSMCs), which can change phenotype by switching from a contractile to a synthetic phenotype (Ailawadi et al., 2009; Shanahan and Weissberg, 1998). These cells can actively alter vessel stiffness by contracting or relaxing. They can also passively alter the mechanics of the AA by mediating cell proliferation,

migration, protein and enzyme synthesis (Mecham et al., 1991; Newby, 2006). The VSMC density distribution in dilated human AA is non-uniform around the ascending aorta (Corte et al., 2006). Such local variations in cell density may alter the local passive and active mechanical properties of the AA and could explain local predisposition in tissue degradation or remodeling capabilities in the outer curvature where dissection and dilation are most likely to occur. In addition, the local effect of the VSMC activation on the regional mechanical properties of ascending aortic tissues has not been reported.

In this study, we investigated if VSMC activation had a significant effect on the mechanical behavior of the pig AA, if the effect was the same around the vessel circumference and if these local variations correspond to the local distribution of VSMCs.

2. Materials and methods

2.1. Pig aortic tissue

All animal tissues were collected in compliance with the Guide for the Care and Use of Laboratory Animals, published by the National Institutes of Health (NIH

* Corresponding author at: Department of Chemical Engineering, McGill University, Wong Building, 3610 University Street, Montreal, Quebec, Canada H3A 2B2. Tel.: +1 514 398 4270; fax: +1 514 398 6678.
  E-mail address: richard.leask@mcgill.ca (R.L. Leask).

Publication no. 8523, revised 1996). The local institutional ethical committee on animal care approved all procedures.

Eleven AA rings were excised from 11 young pigs (4.5 ± 0.5 months old; 43.5 ± 6.7 kg) with an *ex vivo* diameter of 17.4 ± 2.2 mm. Mechanical experiments were carried out within 2 h of collection to preserve VSMC viability.

Two square samples of 15×15 mm were collected from each aortic ring at two locations: inner curvature (ic) and outer curvature (oc), Fig. 1A.

2.2. Biaxial tensile testing

Biaxial tensile tests were conducted using the EnduraTEC *elf* 3200 system (Bose Corporation, Minnesota, USA). Hook-shaped needles were used to attach the sample to the biaxial tensile tester, Fig. 1B. All samples were tested in Krebs–Ringer solution maintained at 37 °C and bubbled with a gas mixture of 95% O_2–5% CO_2. The equi-biaxial testing consisted of 8 cycles of preconditioning and one experimental run from 0% to 30% strain (Green strain) at a displacement rate of 0.1 mm/s. A marker tracking system was used to compute Green strain tensor.

A first biaxial tensile test was performed with the VSMCs in a relaxed state: passive biaxial testing. Then phenylephrine (PE 10^{-5} M) was added in the bath. A second biaxial test was performed after VSMCs reached maximum contraction: active biaxial testing. All samples were fixed in 10% formalin until processed for histological staining quantify the VSMC density.

2.3. Mechanical data analysis

Second Piola–Kirchhoff stress–Green strain curves were generated for the inner curvature and outer curvature in both the circumferential and axial directions and under passive and active testing. The incremental modulus of elasticity (E) was computed at low (7.5%) and high (25%) strain values, Fig. 1C. These strain values were based on our previous study (Choudhury et al., 2009).

To quantify the contribution of VSMCs to the stiffness, we compared the stiffness resulting from the passive testing (E_{pass}) with the active testing (E_{act}) and computed the stiffness increase (SI) expressed as a percentage change. A positive SI indicates a higher stiffness during active testing than passive testing. We have defined the SI as follows:

$$SI = \frac{E_{act} - E_{pass}}{E_{pass}} \times 100$$

The maximum contractile stress (MCS) generated by the tissue when stimulated with PE was computed as the maximum force generated by the tissue divided by the unloaded tissue area in each direction: MCS_{axial} and MCS_{circum}. Unfortunately, we were only able to measure circumferential and axial stresses, therefore it was impossible for us to compute the principal stresses. The maximum contractile stress resultant magnitude (MCSRM) was computed using the Euclidean norm:

$$MCSRM = \sqrt{(MCS_{axial})^2 + (MCS_{circum})^2}$$

We also calculated the angle of the MCS resultant (MCSR) with the circumferential direction (θ_{MCSR}). An angle of 0° and 90° correspond in having the MCSR aligned in the circumferential and axial direction, respectively. The angle value was calculated as follows:

$$\theta_{MCSR} = \arctan\left(\frac{MCS_{axial}}{MCS_{circum}}\right)$$

2.4. VSMC quantification

VSMC nuclei were stained using a hematoxylin–phloxine–saffron (HPS) stain. We manually counted the number of VSMCs in a 0.5 mm² field from 8 fields per sample.

2.5. Statistical analysis

All statistical analyses were performed using GraphPad Prism version 5 (GraphPad Software, San Diego, CA, USA). All statistics are presented as mean values $\pm$ standard deviations. Differences were considered significant for *P*-values < 0.05.

3. Results

3.1. Stiffness increase

VSMC activation significantly increases tissue stiffness (*P*-value < 0.05, one sample test-*t*, significantly different from zero), Fig. 2. This increase was significantly more evident at low strain compared to high strain in both testing directions (*P*-value < 0.001, paired *t*-test). The increase in stiffness in the circumferential direction was significantly greater than the increase in axial stiffness at low strain (*P*-value < 0.01, paired *t*-test) but not significant at high strain (*P*-value=0.113, paired *t*-test).

3.2. Stress response during maximal VSMC contraction

On an average, the circumferential component of the maximum contractile stress (MCS) was significantly higher than in the axial component (*P*-value < 0.001, paired *t*-test), Fig. 3A. Locally, we found that the inner curvature exerted a significantly greater stress than the outer curvature in the circumferential direction (*P*-value < 0.01, paired *t*-test). However, no significant variations were found in the axial direction.

Overall, the MCSR was significantly different between the inner and outer curvature with the inner curvature exerting the highest contraction stress (*P*-value < 0.01, paired *t*-test), Fig. 3B.

Fig. 3C shows the significant difference in the orientation of the MCSR between the inner and outer curvature (*P*-value < 0.01, paired *t*-test). The MCSR was oriented closer towards the circumferential direction in the inner curvature whereas in the outer curvature it was more aligned in the axial direction. Although we did not measure the physical orientation of the cells, the orientation of the MCSR provides information on the contractile force orientation. We found a significantly higher density of VSMCs in the outer curvature (*P*-value < 0.01, paired *t*-test), Fig. 3D.
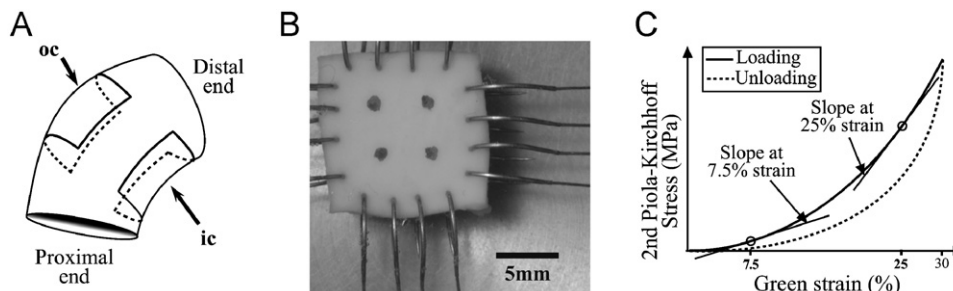

Fig. 1. (A) Locations where the inner curvature and outer curvature samples were taken from the ascending aortic rings. (B) Sample attached with hook-shaped stainless steel needle and silk thread to the biaxial tensile tester. The painted markers on the endothelium surface were used for optical tracking of tissue strain. (C) Typical loading–unloading curve shape illustrating both stiffness values at a low and high strain region.
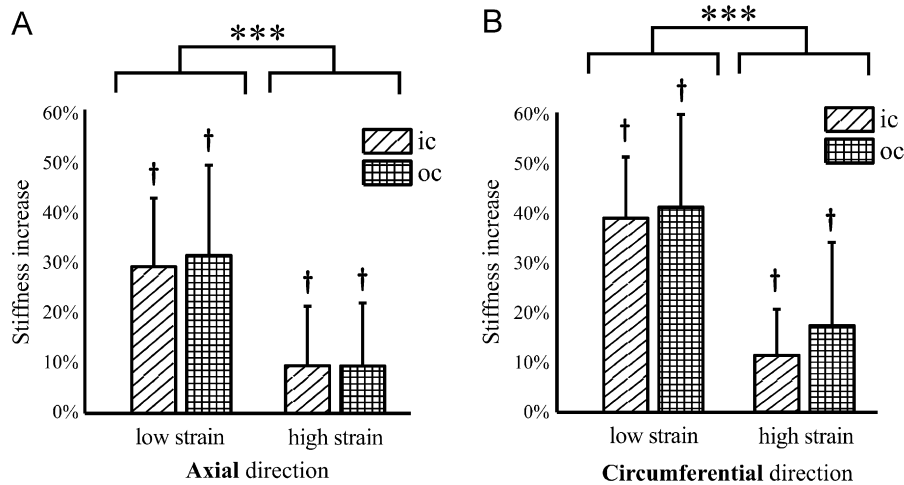
Fig. 2. Stiffness increase at low and high strain at each location in the (A) axial direction and (B) circumferential direction. On average, the stiffness increase was significantly greater at low strain than high strain, ***P-value < 0.001, paired t-test. VSMCs significantly increase tissue stiffness in all locations, strain values and directions, †P-value < 0.05, one sample test-t, significantly different from zero.
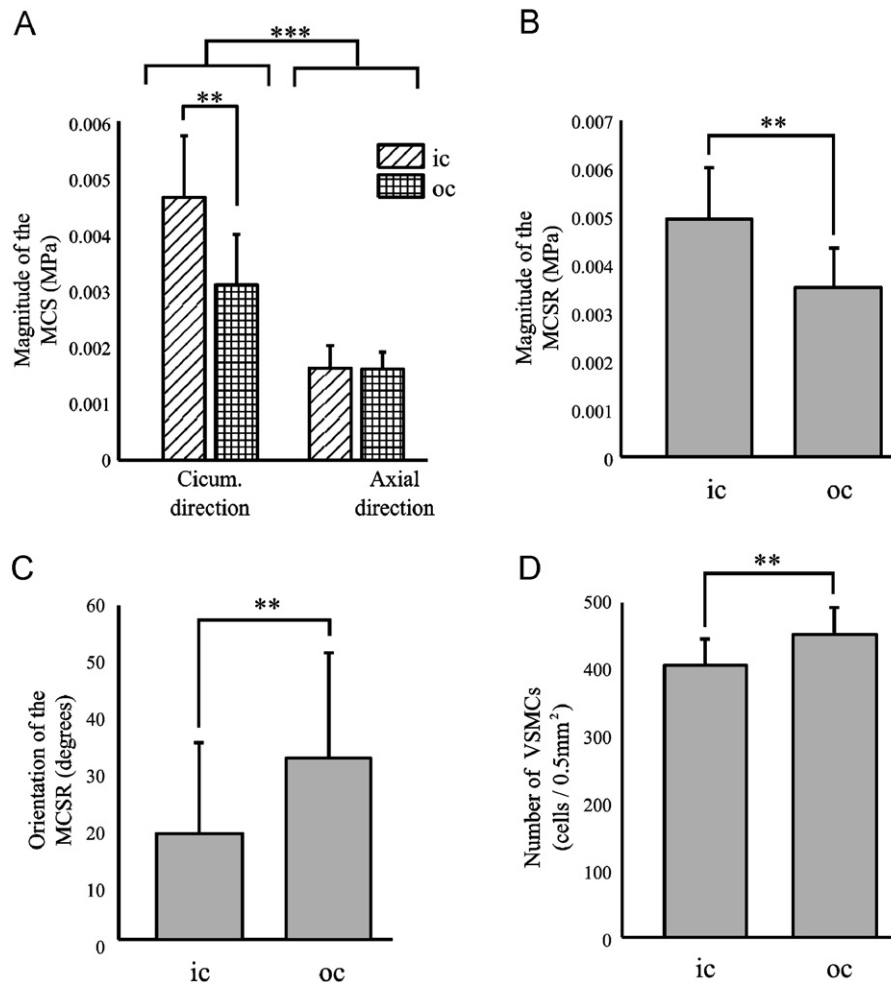

Fig. 3. (A) Magnitude of the maximum contractile stress (MCS) exerted by the tissue during constriction under 10^{-5} M phenylephrine at each location in all testing directions. On average, the MCS exerted in the circumferential direction was significantly higher than in the axial direction (***P-value < 0.001, paired t-test). (B) Magnitude of the MCSR calculated from the axial and circumferential components at each location. (C) Angle between the MCSR and the circumferential axis; a zero angle represents a MCSR oriented toward the circumferential direction. (D) Number of VSMCs present at each location. **P-value < 0.01, paired t-test.

4. Discussion

We observed that the effect of VSMC activation is non-negligible and can increase both the circumferential and axial

stiffness of the tissue. Also, the contribution of VSMCs to local AA stiffness diminishes with increasing strain, Fig. 2. This behavior is in agreement with the work of Cox (1975) on canine carotid and iliac artery and can be explained by the diminishing probability of

having overlapping actin and myosin filaments with strain and leads to a slow loss of the tissue contractile properties (Dobrin, 1978).

The angle values of the MCSR (θ_{MCSR}) are in agreement with the values found by O'Connell et al. (2008) from confocal and electron microscopy image analysis of VSMC orientation. More importantly, we found significant variations in angles between locations where the MCSR was more tilted towards the axial direction in the outer curvature than the inner curvature, Fig. 3C. Beller et al. (2008) found that the aortic root displacement increases the longitudinal stress in the AA at the outer curvature, which can explain the preferential axial VSMC orientation at this location. In addition, we found an increased VSMC density at the outer curvature, which again supports the hypothesis of a remodeling response to increased strain/stress, which has been shown to regulate the VSMC proliferation (Jiang et al., 2009).

Regional variations in VSMC orientation and density also suggest a local predisposition in the remodeling capacities of the tissue at the outer curvature, which could lead to heterogeneous variation in stiffness around the circumference of older pig AA as it has been observed in human (Choudhury et al., 2009). In addition, the increased stress/strain at this location could have an effect on the transitional phenotype change in the VSMCs. Aneurysmal tissue have an increased expression of osteopontin in the media, which indicates the transition of VSMCs from a contractile phenotype to a synthetic phenotype (Lesauskaite et al., 2001). This phenotype change could increase the production of matrix metalloproteinases (Ailawadi et al., 2009; Lesauskaite et al., 2001; Shanahan and Weissberg, 1998) and degrade elastin and collagen responsible for the structural integrity of the walls and thus leading to structural weakening and aneurysm formation. The reduced contractile strength of the outer curvature, Fig. 3B, despite the increased cell density, Fig. 3D, supports the hypothesis of more synthetic VSMCs on the outer wall.

Conflict of interest statement

All authors disclose any financial and personal relationships with other people or organizations that could inappropriately influence (bias) their work.

Acknowledgements

References

Ailawadi, G., Moehle, C.W., Pei, H., Walton, S.P., Yang, Z., Kron, I.L., Lau, C.L., Owens, G.K., 2009. Smooth muscle phenotypic modulation is an early event in aortic aneurysms. Journal of Thoracic and Cardiovascular Surgery 138 (6), 1392–1399.

Beller, C.J., Labrosse, M.R., Thubrikar, M.J., Robicsek, F., 2008. Finite element modeling of the thoracic aorta: including aortic root motion to evaluate the risk of aortic dissection. Journal of Medical Engineering and Technology 32 (2), 167–170.

Choudhury, N., Bouchot, O., Rouleau, L., Tremblay, D., Cartier, R., Butany, J., Mongrain, R., Leask, R.L., 2009. Local mechanical and structural properties of healthy and diseased human ascending aorta tissue. Cardiovascular Pathology 18 (2), 83–91.

Corte, A.D., Santo, L.S.D., Montagnani, S., Quarto, C., Romano, G., Amarelli, C., Scardone, M., Feo, M.D., Cotrufo, M., Caianiello, G., 2006. Spatial patterns of matrix protein expression in dilated ascending aorta with aortic regurgitation: congenital bicuspid valve versus Marfan's syndrome. Journal of Heart Valve Disease 15 (1), 20–27.

Cotrufo, M., Corte, A.D., Santo, L.S.D., Feo, M.D., Covino, F.E., Dialetto, G., 2003. Asymmetric medial degeneration of the ascending aorta in aortic valve disease: a pilot study of surgical management. Journal of Heart Valve Disease 12 (2), 127–133.

Cox, R.H., 1975. Arterial wall mechanics and composition and the effects of smooth muscle activation. American Journal of Physiology 229 (3), 807–812.

Desai, M.Y., White, R.D., Bluemke, D.A., Lima, J.A.C., 2007. Cardiovascular magnetic resonance imaging. In: Topol, E.J. (Ed.), Textbook of Cardiovascular Medicine. Lippicott Williams and Wilkins, Philadelphia, pp. 897–930.

Dobrin, P.B., 1978. Mechanical properties of arterises. Physiological Reviews 58 (2), 397–460.

Gomez, D., Zen, A.A.H., Borges, L.F., Philippe, M., Gutierrez, P.S., Jondeau, G., Michel, J.B., Vranckx, R., 2009. Syndromic and non-syndromic aneurysms of the human ascending aorta share activation of the Smad2 pathway. Journal of Pathology 218 (1), 131–142.

Jiang, X., Austin, P.F., Niederhoff, R.A., Manson, S.R., Riehm, J.J., Cook, B.L., Pengue, G., Chitaley, K., Nakayama, K., Nakayama, K.I., Weintraub, S.J., 2009. The mechanoregulation of proliferation. Molecular Cell Biology 29 (18), 5104–5114.

Lesauskaite, V., Tanganelli, P., Sassi, C., Neri, E., Diciolla, F., Ivanoviene, L., Epistolato, M.C., Lalinga, A.V., Alessandrini, C., Spina, D., 2001. Smooth muscle cells of the media in the dilatative pathology of ascending thoracic aorta: morphology, immunoreactivity for osteopontin, matrix metalloproteinases, and their inhibitors. Human Pathology 32 (9), 1003–1011.

Mecham, R.P., Stenmark, K.R., Parks, W.C., 1991. Connective tissue production by vascular smooth muscle in development and disease. Chest 99 (3 Suppl), 43S–47S.

Newby, A.C., 2006. Matrix metalloproteinases regulate migration, proliferation, and death of vascular smooth muscle cells by degrading matrix and non-matrix substrates. Cardiovascular Research 69 (3), 614–624.

O'Connell, M.K., Murthy, S., Phan, S., Xu, C., Buchanan, J., Spilker, R., Dalman, R.L., Zarins, C.K., Denk, W., Taylor, C.A., 2008. The three-dimensional micro- and nanostructure of the aortic medial lamellar unit measured using 3D confocal and electron microscopy imaging. Matrix Biology 27 (3), 171–181.

Shanahan, C.M., Weissberg, P.L., 1998. Smooth muscle cell heterogeneity: patterns of gene expression in vascular smooth muscle cells in vitro and in vivo. Arteriosclerosis Thrombosis and Vascular Biology 18 (3), 333–338.